Modelling Fast-moving Flow-like Landslides by Cellular Automata: Simulations of Debris Flows and Lahars

V. LUPIANO[1], G. MACHADO[2,3], G.M. CRISCI[1], S. DI GREGORIO[2]
[1]Dept. of Biology, Ecology, Earth Science, University of Calabria, Arcavacata, 87036 Rende, Italy
{valeria.lupiano, crisci}@unical.it
[2]Dept. of Mathematics and Computer Science, University of Calabria, Arcavacata, 87036 Rende, Italy
salvatore.digregorio@unical.it, machado@mat.unical.it
[3]Faculty of Engineering, National University of Chimborazo, 060150 Riobamba, Ecuador
gmachado@unach.edu.ec

Abstract: - Cellular Automata (CA) represent a computational paradigm for complex fluid-dynamical phenomena that evolve on the basis on local interactions. Macroscopic CA (MCA) characterize a methodological approach for modelling and simulating large scale (extended for kilometers) surface flows. Fast-moving flow-like "landslides", as lahars, debris and mud flows, represent very destructive natural disasters as number of casualties in the world. Simulation of such phenomena could be an important tool for hazard management in threatened regions. This paper presents shortly the modelling methodology of MCA for such type of surface flow together with the models SCIDDICA-SS2, SCIDDICA-SS3 (both for debris, mud and granular flows) and LLUNPIY (for primary and secondary lahars) together with their significant applications in simulating both past and probable future events. At the end, a new result about possible hazard of Cotopaxi volcano is reported; the repetition of the 1877 catastrophic lahar invasion is simulated, beginning from the immediate melting of part of the Cotopaxi icecap because of volcanic activity.

Key-Words: - Modeling, Simulation, Cellular Automata, Lahars, Debris flow, Natural Hazard

1 Introduction

John von Neumann conceived Cellular Automata at the end of the 1940s on suggestion of Stanislaw Ulam, for the purpose of studying the formal (and computational) properties of self-reproducing organisms, with the most general notion of self-reproduction in mind, to be combined with the notion of universal calculability [27]. Interest in CA by the scientific community had been intermittent, but today they have been firmly established as a parallel calculation model and a tool to model and simulate complex phenomena.

CA are spatially and temporally discrete, abstract computational systems that can exhibit chaotic behavior, self-organization and lend themselves to description in rigorous mathematical terms, these have proven useful both as general models of complexity of non-linear dynamics, in a diversity of scientific fields. The computational model of the growth of a snowflake is an example of the CA. It is represented by a uniform array of numerous identical cells, where each cell may assume only a few states and interact with only a few adjacent cells. The elements of the system (the cells and the rule to calculate the subsequent state of a cell) can be very simple, yet nonetheless give rise to a notably complex evolution [16].

In its essential description, CA can be seen as a space, partitioned in cells, each one embedding an identical input/output computing unit. Each cell is characterized by its state. S is the finite set of the states. Input for each cell is local and is given by the states of m neighboring cells, where the neighborhood conditions are given by a pattern invariant in time and space. At time 0, cells are in arbitrary states (initial conditions of system) and the CA evolves changing simultaneously the state at discrete times, according to local evolution rules, which are functions of the states of the cell itself and its neighbors.

Since the self-reproduction cellular automata, CA is widely applied to various fields of arts, biology, chemistry, communication, cultural heritage, ecology, economy, geology, engineering, medicine, physics, sociology, traffic control, etc.

In the last years, the research into simulations of CA in fluid dynamics, as an important field for Cellular Automata applications, is accelerating in many directions. The most obvious research direction has been the attempts of simulating flow-type landslides that have been carried out by several

authors with satisfactory results (e.g., [7, 10, 25]). An extension of the CA paradigm for macroscopic systems and a related modeling methodology were established in order to simulate also fluid-dynamical phenomena [14]. Good simulations results were obtained for some types of "macroscopic" surface flows, for instance, lava flows and pyroclastic flows for volcanic eruptions, debris, mud, granular flows for landslides with the SCIDDICA, SCIARA, PYR, and models respectively [3, 11, 12].

In this context, the next section considers the MCA general frame for modeling macroscopic surface flow, an extended definition of *CA* for modeling macroscopic phenomena that can be framed in an acentric context, developing CA alternative strategies, which are reported in the subsequent sections. Afterward, the three cellular models SCIDDICA-SS2 [4], SCIDDICA-SS3 [6] and LLUNPIY [20], concerning respectively debris flows and lahars are exposed together with simulation examples of real cases. Comments and conclusions are reported at the end.

2 MCA General Frame

The applications of CA to fluid dynamics have generated two important computational paradigms: the *Lattice Gas* models [15], and from there, the more robust *Lattice Boltzmann method* [9, 26]. However, many complex macroscopic phenomena seem to be difficult to model with these types of CA, since they occur on a very broad spatial scale. Consequently, a macroscopic level of description must be used, which implies, however, the management of a large quantity of data, e.g. morphological data. It is hence unthinkable to work at the microscopic level, where evaluation factors such as data quality would make no sense. The move to the macroscopic also means a greater number of states, which could also lead to complicated transition functions that can no longer be practically identified with a lookup table, as in the microscopic one.

The classical CA definition is not sufficient for modelling spatially extended natural macroscopic phenomena [2]. This extension in its completeness does not formally alter the classic notion of CA as developed by von Neumann, but renders it capable of modeling and dealing with the complex macroscopic phenomena to be simulated. A very high number of states are needed for macroscopic phenomena, because they must contain all the information related to the portion of space corresponding to the cell, with all the specifications needed to model the evolution of the phenomenon of interest. This gives rise to a very high number of states, which can be formally represented in terms of sub-states (i.e., the Cartesian product of the sets of all the sub-states constitutes the set of the states). In this way, a sub-state specifies important characteristics (e.g., altitude, temperature, etc.) to be attributed to the state of the cell and necessary to determine the evolution of the CA**.**

2.1 CA Criteria for modeling of macroscopic phenomena.

The extended definition of CA for modeling macroscopic phenomena descends from the need to correlate the evolution of the phenomenon with the evolution of the simulation; it is necessary also to consider, those simple, non-local specifications (the parameters) related to the phenomenon or its representation in terms of CA (Etnean lava solidification temperature, cell dimension, etc.).

A CA is formally defined as a septuplet:

$$\langle R, G, S, X, P, \tau, \gamma \rangle$$

when its components are specified as follows.

2.1.1 Global parameters

The abstract *CA* must be uniquely related to the real macroscopic phenomena with regard to time and space.

Some global parameters must be considered: at least

- the cell dimensions e.g. the distance between the centers of two neighboring cells p_d;
- the time corresponding to one step of the transition function p_t;

$P = (p_d, p_t, \ldots.)$ is the finite set of global parameters that affect the transition function.

2.1.2 Space

The cell normally corresponds to a portion of space; therefore, the cellular space should be three-dimensional: $R = \{(x,y,z) \mid x,y,z \in N\}$ with $0 \le x \le l_x$, $0 \le y \le l_y$, $0 \le z \le l_z$, is the set of coordinates integer points that define the finite region of the space where the phenomenon evolves. $\boldsymbol{N}$ is the set of natural numbers.

If there are legitimate simplifications, it is easy to reduce the formula to 1-2 dimensions.

2.1.3 Sub-states

The macroscopic part of the phenomenon may imply heterogeneity. Each characteristic significant to the evolution of the system and related to the portion of space corresponding to the cell is identified as a sub-state; the Cartesian product of the

ISBN: 978-1-61804-314-6

sets of sub-states expresses the finite set S of the states:

$$S = S_1 \times S_2 \times \ldots\ldots \times S_n$$

The value of a sub-state is approximated to a unique value in the space occupied by the cell (e.g. the temperature).

When a characteristic (e.g., a physical quantity) is expressed as a continuous variable, then a finite but sufficient number of meaningful digits are used so that the set of possible values can be arbitrarily large but finite.

The cellular space should be three-dimensional, but a reduction to two dimensions is permitted if the quantity related to the third dimension (height) can be represented as sub-states of the cell: this is the case with surface flows, which include debris flows, mudflow, granular flows and lahars.

2.1.3 "Elementary" Processes

Just as the state of the cell can be broken down into sub-states, the transition function τ can be subdivided into "elementary" processes, defined by the functions $\sigma_1, \sigma_2 \ldots . \sigma_k$ with k being the number of elementary processes.

The elementary processes are applied sequentially according to a defined order. Different elementary processes can result in a different neighborhood. Each elementary process updates the states of the CA.

2.1.4 Neighborhood

$X=\{\xi_0, \xi_1, \ldots\ldots \xi_{m-1}\}$, the neighborhood relationship (or index), is a finite set of three-dimensional vectors, that specifies the cells belonging to the neighborhood by addition of co-ordinates of the considered cell, the so called central cell. The union of all neighborhoods associated with each elementary process specifies the CA neighborhood.

2.1.5 External influences

Sometimes, a sort of input from the "external world" on the cells of the *CA* must be considered; these account for external influences that cannot be described in local terms (e.g., the rainfall) for simulating on the base of real or probabilistic data. Therefore, special and/or additional functions (γ) must be specified for that type of cell (G). γ and G do not need to be always specified in the CA models.

2.2 Algorithm of Minimization of Differences

Many complex systems evolve locally toward conditions of maximum possible equilibrium: essentially in terms of *CA*, the system tends to minimize, within the neighborhood, differences related to a certain amount of matter, giving rise to flows from central cell to the other neighbor cells [1, 14].

In the context of *CA*, this means that sub-states "outflow" have to be calculated for the generic cell c from the "distributable" quantity q_d. Values of such outflows correspond to values of the sub-states "inflow" for c neighbors in the next step. τ is applied simultaneously on each cell in R and flows, potentially from each cell toward neighborhood cells, give rise to the evolution of the system.

2.2.1 Explicatum of the minimization problem

Definitions:

$n = \#X$;

q_d = distributable quantity in the central cell;

q_0 = not distributable quantity in the central cell;

q_i = quantity in the cell i $1 \le i < n$;

f_0' is the part of q_d remaining in the central cell;

f_i' = flow from the central cell towards the cell i $1 \le i < n$;

$q_i' = q_i + f_i'$ $0 \le i < n$;

Bound: $q_d = \Sigma_{0 \le i < n} f_i'$;

Problem: f_h' $0 \le h < n$ must be determined in order to minimize the sum of all q differences between all the pairs of cells in the neighborhood:

$$\Sigma_{\{(i,j)|0 \le i < j < n\}} \left| q_i' - q_j' \right| \qquad (1)$$

2.2.2 Minimization of the Differences

Initialization:

a) all the neighboring cells are considered "admissible" to receive flows from the central cell, A is the set of admissible cells.

Cycle:

b) the "average q" (av_q) is found for the set A of admissible cells:

$$av\_q = (q_d + \Sigma_{i \in A} q_i) / \#A. \qquad (2)$$

c) each cell x with $q_x \ge av\_q$ is eliminated from the set A. It implies that "average q" does not increase, because:

$$\begin{aligned} av\_q &= (q_d + \Sigma_{i \in A} q_i) / \#A = \\ &= (q_d + \Sigma_{i \in A} q_i - av\_q) / (\#A - 1) \ge \\ &\ge (q_d + \Sigma_{i \in A} q_i - q_x) / (\#A - 1) \end{aligned} \qquad (3)$$

End of cycle:

d) go to step-b until no cell is eliminated.

Result:

e) $f_i' = av\_q - q_i$ for $i \in A$ $(q_i < av\_q)$;
$f_i' = 0$ for $i \notin A$ $(q_i' \ge av\_q)$

Conservation bound:

$$\Sigma_{i\in A} f_i' = \Sigma_{i\in A}(av\_q - q_i) = \quad (4)$$
$$= \#A(q_d + \Sigma_{i\in A} q_i) / \#A - \Sigma_{i\in A} q_i = q_d$$

Properties:

P1: $q_i' = f_i' + q_i = av\_q - q_i + q_i = av\_q$ for $i \in A$

P2: $q_i' = q_i$ because $f_i' = 0$ for $i \notin A$

2.3 Validation phase of MCA models

Two main phases are involved for verifying the reliability of MCA simulation models: the calibration phase identifies an optimal set of parameters capable of adequately reproduce the observed event; the validation phase, in which the model is tested on a sufficient (and different) number of cases similar in terms of physical and geomorphologic properties. Once the optimal set of parameters is calibrated, the model can be considered applicable in the same homogeneous geological context in which the parameters are derived, enabling a predictive analysis of surface flow hazard.

The likelihood between the cells involved by the real event and the cells involved in the simulation can be measured by the fitness function in relation to the dimensions *d* of cellular space:

$$f(R,S) = \sqrt[d]{\frac{R \cap S}{R \cup S}} \quad (5)$$

where *R* is the set of cells involved in the real event and *S* is the set of cells involved in the simulated event. This function ranges from **0** (completely wrong simulation) to **1** (perfect match between real and simulated events); values greater than **0.7** may be considered acceptable for two dimensions.

3 The Model SCIDDICA-SS2

This version of SCIDDICA is an extension of model applied to the landslides of Sarno [13]. Such an extension involves more sub-states, processes and parameters because the phenomenon is more complex [5]. In fact, the most sophisticated version SS2 is shortly presented together with the simulation of the combined subaerial-subaqueous part of Albano landslide (Rome, Italy).

3.1Main features of SCIDDICA-SS2

The hexagonal CA model SCIDDICA-SS2 is the quintuple $\langle R, X, S, P, \tau \rangle$:

- R is the set of regular hexagons covering the region, where the phenomenon evolves.
- X identifies the geometrical pattern of cells, which influence any state change of the central cell: the central cell (index 0) itself and the six adjacent cells (indexes 1,…6)
- S is the fine set of states of the fine automaton, it is equal to the Cartesian product of the sets of the considered sub-states (Table 1).
- P is the set of global physical and empirical parameters, which account for the general frame of the model and the physical characteristics of the phenomenon (Table 2).
- $\tau: S^7 \rightarrow S$ is the deterministic state transition function; its elementary processes are shortly summarized in the next section.

Table 1. Subs-states

Sub-states	Description
S_A, S_D	cell **A**ltitude, the maximum **D**epth of detrital cover.
S_{TH}	the average **T**hickness **H**ead of landslide debris inside the cell
S_{KH}	the debris **K**inetic **H**ead
S_X, S_Y	the co-ordinates **X** and **Y** of the lahar barycenter inside the cell
S_E, S_{EX}, S_{EY}, S_{KHE} (6 components)	the part of debris flow (**E**xternal flow), **E**xternal flow co-ordinates **X** and **Y**, the debris kinetic head
S_I, S_{IX}, S_{IY}, S_{KHI} (6 components)	the part of debris flow toward the adjacent cell (**I**nternal flow), **I**nternal flow co-ordinates **X** and **Y**, **K**inetic **H**ead of **I**nternal flow

Table 2. Physical and empirical parameters

Parameters	Description
p_a, p_t	cell **a**pothem, **t**emporal correspondence of a CA step
p_{adhw}, p_{adha}	the **w**ater/**a**ir **adh**esion values
p_{fcw}, p_{fca}	the **w**ater/**a**ir **f**riction **c**oefficient for debris outflows
p_{tdw}, p_{tda} p_{edw}, p_{eda}	**w**ater/**a**ir parameters for energy **d**issipation by **t**urbulence and by **e**rosion respectively
p_{ml}	the **m**atter **l**oss in percent when the debris enters into water
p_{mtw}, p_{mta}	the **w**ater/**a**ir activation **t**hresholds of the **m**obilization
p_{tmt}	the activation **t**hreshold of the **m**obilization for the **t**ransept
p_{pew}, p_{pea}	the **w**ater/**a**ir **p**rogressive **e**rosion parameters
p_{wr}	the **w**ater **r**esistance parameter

3.2 SCIDDICA-SS2 transition function

In the following, a sketch of the local elementary processes will be given, in order to capture the mechanisms of the transition function; the execution of an elementary process updates the sub-states.

ISBN: 978-1-61804-314-6

Variables concerning sub-states and parameters are indicated by their subscript. When sub-states need the specification of the neighborhood cell, their index is indicated between square brackets. ΔQ means variation of the sub-state S_Q.

3.2.1 Mobilization effects

When the kinetic head value overcomes an opportune threshold ($KH>mt$) depending on the soil features and its saturation state then a mobilization of the detrital cover occurs proportionally to the quantity overcoming the threshold:

$$pe\cdot(KH-mt) = \Delta TH = -\Delta D \quad (6)$$

(the detrital cover depth diminishes as the debris thickness increases), the kinetic head loss is:

$$-\Delta KH = ed\cdot(KH-mt) \quad (7)$$

3.2.2 Turbulence effect

The effect of the turbulence is modelled by a proportional kinetic head loss at each SCIDDICA step: $-\Delta KH=td\cdot KH$.

3.2.3 Debris outflows

Outflows computation is performed in two steps: determination of the outflows by the Algorithm for the Minimization of Differences (AMD [14]) applied to "heights" of the cell neighborhood and determination of the shift of the outflows [2].

SCIDDICA-SS2 involves a type of alteration of data regarding the height values in order to account for run-up effects concerning kinetic energy, expressed by kinetic head.

Terms of AMD are the height (h) of cells in the neighborhood, to be minimized by flows (f), whose sum is equal to the quantity q to be distributed in the neighborhood cells.

$$h[0] = A[0] + KH[0] + adh \quad (8)$$

$$h[i] = A[i]+TH[i], 1\leq i\leq 6) \quad (9)$$

$$q = TH[0] - adh = \Sigma_{0\leq i\leq 6} f[i] \quad (10)$$

AMD application minimizes

$$\Sigma_{\{(i,j)\,|\,0\leq i<j\leq 6\}}(|(h[i]+f[i]) - (h[j]+ f[j])|) \quad (11)$$

The barycenter co-ordinates x and y of moving quantities are the same of all the debris inside the cell and the form is ideally a "cylinder" tangent the next edge of the hexagonal cell. An ideal distance "d" is considered between the central cell debris barycenter and the center of the adjacent cell i including the slope $\theta[i]$.

The $f[i]$ shift "sh" is computed for debris flow according to the following simple formula, which averages the movement of all the mass as the barycenter movement of a body on a constant slope with a constant friction coefficient:

$$sh = v\cdot t + g\cdot(\sin\theta - fca\cdot\cos\theta)\cdot t^2/2 \quad (12)$$

with "g" the gravity acceleration, the initial velocity

$$v = \sqrt{(2g\cdot KH[0])} \quad (13)$$

The motion involves three possibilities: (1) only internal flow, i.e., the shifted cylinder is completely inside the central cell; (2) only external flow, all the shifted cylinder is inside the adjacent cell; (3) the shifted cylinder is partially internal to the central cell, partially external to the central cell, the flow is divided between the central and the adjacent cell, forming two cylinders with barycenters corresponding to the barycenters of the internal debris flow and the external debris flow. The kinetic head variation is computed according to the new position of internal and external flows, while the energy dissipation was considered as a turbulence effect in the previous elementary process.

3.2.4 Flows Composition

When debris outflows are computed, the new situation involves that external flows left the cell, internal flows remain in the cell with different co-ordinates and inflows (trivially derived by the values of external flows of neighbor cells) could exist. The new value of TH is given, considering the balance of inflows and outflows with the remaining debris in the cell. A kinetic energy reduction is considered by loss of flows, while an increase is given by inflows: the new value of the kinetic head is deduced from the computed kinetic energy. The co-ordinates determination is calculated as the average weight of X and Y considering the remaining debris in the central cell, the internal flows and the inflows.

3.3 Simulation with SCIDDICA-SS2

SCIDDICA-SS2 was calibrated using the 1997 Albano lake (Italy) debris flow that is a case of combined subaerial-subaqueous event and validated with other five cases occurred on the lake slope [22]. This landslide occurred in the eastern slope of the Albano Lake on the November 7, 1997, after an intense rainfall event, mobilizing about 300 m^3 of alluvial material. Simulations permit to validate the general model and to calibrate adequately its parameters [4, 5]. Fig.1 shows the corresponding simulation concerning subaerial/subaqueous part.

SCIDDICA-SS2 model was also used for a preliminary evaluation of the spatial hazard in the same area [17]: 89 hypothetical debris-flows, including 11 subaqueous ones, were simulated. Hypothetical sources are located at the vertices of a square grid with side length 50m. A simple scene susceptibility (Fig.2) was generated in a GIS

(Geographic Information System) overlaying the paths of simulated flows, both subaerial that subaqueous.

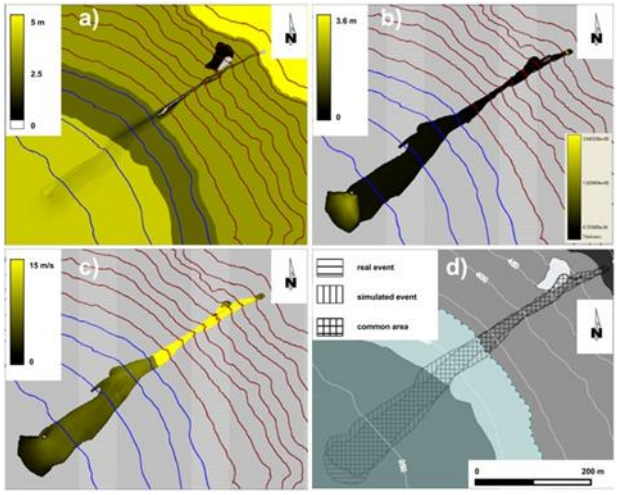

Fig.1: 1997 Albano Lake debris flow. a) eroded regolith; b) final thickness; c) maximum local velocities reached by simulated flows; d) real event compared with SCIDDICA-SS2 simulation.

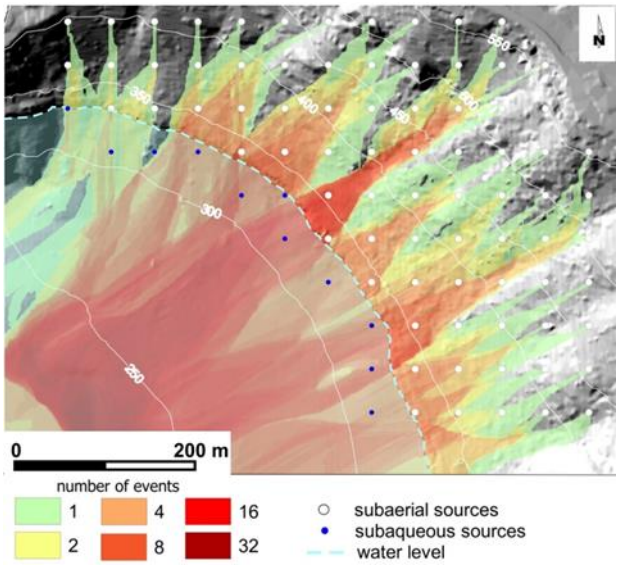

Fig.2: Albano lake susceptibility zonation.

4 The Model SCIDDICA-SS3

One of the latest models of the SCIDDICA family, named SCIDDICA-SS3, inherits all the features of its predecessor SS2 version, in order to improve management of physical conservation laws, in particular, inertial effects that characterize some rapid debris flow [6].

4.1New features of SCIDDICA-SS3

In the SS3 version of SCIDDICA, a better approximation has been introduced for the determination of outflows from a cell towards its adjacent cells, in terms of momentum computation. The following sub-states S_{Mx} and S_{My}, the two components of the debris momentum, are added.

The main difference consists in determination of a further alteration of data regarding the height values; directional effects concerning momentum are expressed by a correction function *corr*, which diminishes the height for cells in the same direction of the momentum and increases the height for cells in the opposite direction. It is applied to computation of minimizing outflows:

$$h[0] = A[0] + KH[0] + adh \quad (13)$$

$$h[i] = A[i]+TH[i] +corr(Mx[0],My[0],1\leq i\leq 6) \quad (14)$$

$$q = TH[0] - adh = \Sigma_{0\leq i\leq 6}\, f[i] \quad (15)$$

Trivial changes of momentum are computed in elementary processes involving energy loss: turbulence effect and mobilization effect.

4.2 Simulation with SCIDDICA-SS3

SCIDDICA-SS3 was calibrated using the 1997 Albano lake event [6]. In addition, SS3 version was applied for simulating 2009 debris flows in Giampilieri Superiore in Messina city territory. On October 1, 2009, almost all the Peloritani Mountains area (NE Sicily) was involved in a rainfall (approximately 17 cm of rain in 180 minutes) with more than 500 landslides.

Fig.3 shows a good simulation of debris flows that describe the debris run-out, especially in high zone of slope. Hence, such results may be a base for evaluating debris flow hazard and effects of possible remedial works in this study area [17, 18] and in other area with similar geophysical features.

5 The Model LLUNPIY

Lahars are very complex dynamical systems, very difficult to be modelled: they can grow by soil erosion and/or incorporation of water, along watercourses. Unconsolidated pyroclastic material can be easily eroded by superficial water forming dilute sediment-laden flows, which can bulk-up to debris flows whose magnitude will depend upon the volume of both the water and remobilized material. Volcanic eruptions can generate directly (primary lahars) or indirectly (secondary lahars) catastrophic surface flows that are a mixture of volcanic debris and water occurring on and around volcanoes [21].

LLUNPIY (**L**ahar modelling by **L**ocal rules based on an **UN**derlying **PI**ck of **Y**oked processes, from the Quechua word llunp'iy meaning flood) is a CA model for simulating lahars in terms of complex

system evolving on the base of local interaction. This model inherits all the features of SCIDDICA-SS2 [4, 5].

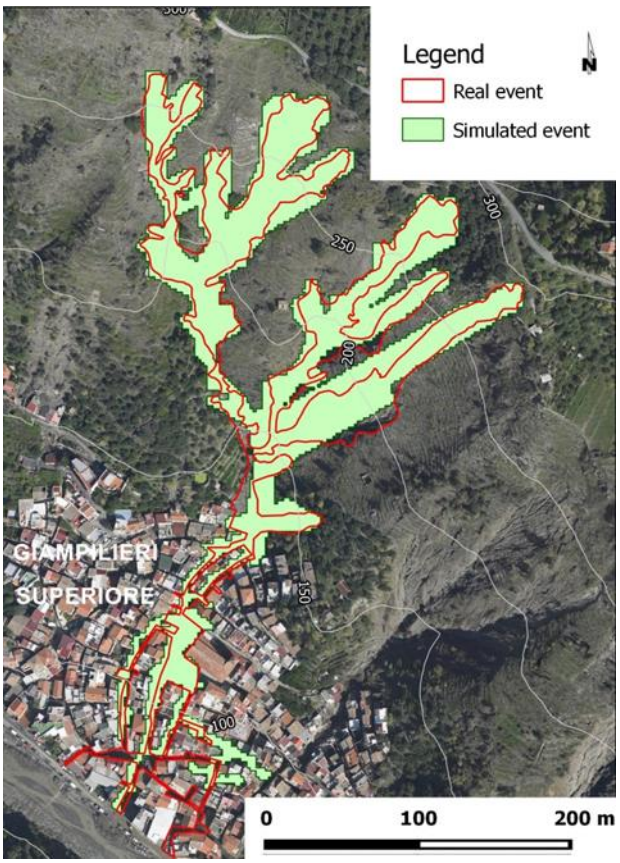

Fig.3: Giampilieri Superiore debris flow compared with SCIDDICA-SS3 simulation

5.1 Formal definition of LLUNPIY

The LLUNPIY model is a two dimensional CA with a hexagonal tessellation and is defined by the septuplet: <R, G, X, S, P,τ, γ>
where:

- $R = \{(x, y): x, y \in \mathbb{N}, 0 \leq x \leq l_x, 0 \leq y \leq l_y\}$ is the set of points with integer co-ordinates, that individuate the regular hexagonal cells;
- G ⊆ R is the set of cells, corresponding to the glacier, where lahar is formed when pyroclastic matter melts ice (the case of primary lahars) or cells effected by rainfall (the case of secondary lahars);
- X = {(0, 0), (1, 0), (0, 1), (−1, 1), (−1, 0), (0,−1), (−1,−1)}, the neighbourhood index, identifies the geometrical pattern of cells, which influence state change of the "central" cell;
- S is the finite set of states of the finite automaton, embedded in the cell; it is equal to the Cartesian product of the sets of the considered sub-states (Table 1).
- P is the set of the global physical and empirical parameters, which account for the general frame of the model and the physical characteristics of the phenomenon (Table 2);
- $\tau: S^7 \rightarrow S$ is the cell deterministic state transition in R, it embodies the SCIDDICA-SS2 elementary processes, furthermore introducing two new ones in order to account to characteristics of the lahar dynamics: the following main components of the phenomenon:
  - σ_{wp}, water percolation;
  - σ_{psm}, pyroclastic stratum mobilization;
  - σ_{wf}, water flow;
  - $\sigma_{wie\&ld}$, water inclusion, extrusion and process of lahar complete deposition

Table 3. Sub-states

Sub-States	*Description*
S_A, $S_{D,}$ (S_{D1}, S_{D2})	cell **A**ltitude, tephra stratum **D**epth; it could be specified if data are available in "**1**" the mobilizable stratum, and "**2**", the only erodible stratum.
S_{SR}, S_{SWC}, S_{MIR}	mobilizable stratum: **S**tratum **R**eceptivity, **S**tratum **W**ater **C**ontent, **M**ax **I**nfiltration **R**ate
S_{WL}, S_{WKH}, S_{WO}	**W**ater **L**evel, **W**ater **K**inetic **H**ead, **W**ater **O**utflows (6 components normalized to a thickness)
S_{IT} , S_{LT}, S_{KH}, S_{LWC}	**I**ce **T**hickness**,** **L**ahar **T**hickness, Lahar **K**inetic **H**ead, **L**ahar **W**ater **C**ontent
S_X, S_Y	the co-ordinates **X** and **Y** of the lahar barycenter inside the cell
S_{MX}, S_{MY},	the components **x** and **y** of the lahar **M**omentum inside the cell
S_E, S_{EX}, S_{EY}, S_{KHE} (6 components)	**E**xternal flow normalized to a thickness, **E**xternal flow co-ordinates **X** and **Y**, **K**inetic **H**ead of **E**xternal flow
S_I, S_{IX}. S_{IY}, S_{KHI} (6 components)	**I**nternal flow normalized to a thickness, **I**nternal flow co-ordinates **X** and **Y**, **K**inetic **H**ead of **I**nternal flow

- γ_1: $\mathbb{N}\times G_g\times S_{IT}\times S_A\times S_{LT} \rightarrow S_{IT}\times S_A\times S_{LT}$ for primary lahars expresses the "external influence" of fall of the pyroclastic matter on glacier (G_g cells) and consequently ice state change in lahar with the addition of pyroclastic matter at the initial CA step. ℕ is here referred to the step number.
- γ_2: $\mathbb{N}\times G\times S_{WL}\times S_{WKH} \rightarrow S_{WL}\times S_{WKH}$ for secondary lahars expresses the raining water quantity to be added for G cells at each CA step. ℕ is here referred to the step number.

ISBN: 978-1-61804-314-6

Table 4: Physical and empirical parameters.

Parameters	Description
p_a p_t	cell **a**pothem, **t**emporal correspondence of a CA step
p_{fc}	**f**riction **c**oefficient parameter
p_{td} p_{ed} p_{pe} p_{mt}	lahar parameters: **t**urbulence **d**issipation and **e**rosion **d**issipation of energy; lahar parameter of **p**rogressive **e**rosion, **m**obilization **t**hreshold
p_{slt} p_{wct}	slope threshold, **w**ater **c**ontent **t**hreshold
p_{khl}	**k**inetic **h**ead **l**oss
p_{dft} p_{adh1} p_{adh2}	lahar complete **d**eposit **f**ormation **t**hreshold, minimum **adh**erence, maximum **adh**erence

5.2 The specific LLUNPIY elementary processes

5.2.1 σ_{wp}, water percolation

Part of water from rainfall infiltrates in the mobilizable stratum, that may be considered as a water reservoir of a given capacity, that is the sum of stratum water receptivity S_{SR} plus stratum water content S_{SWC}; a maximum infiltration rate (in a step) S_{MIR} is fixed according to the cell physical characteristics related to the mobilizable stratum. Infiltration v_I is the minimum value among S_{WL}, S_{SR} and S_{MIR}. Sub-states are updated:

$S_{WL}' = S_{WL} - v_I \quad S_{SR}' = S_{SR} - v_I \quad S_{SWC}' = S_{SWC} + v_I$

5.2.2 σ_{psm}, pyroclastic stratum mobilization

The saturation conditions of pyroclastic stratum are specified by overcoming two thresholds, that regard the percent of S_{SWC} related to water capacity of the mobilizable stratum and a sufficient slope angle α_i related to some adjacent cell i $(1 \le i \le 6)$ such that the slope component of gravity force is larger than the reduced cohesion forces:

$S_{SWC} / (S_{SWC} + S_{SR}) > p_{wct} \quad \arctan(\alpha_i) > p_{slt}$

When saturation conditions occur, the mobilizable stratum liquefies after the collapse of soil cohesion forces and encloses the surface water; then:

$S_{LT}'=S_{D1}+S_{WL}-S_{SR}; \quad S_{LWC}'=(S_{SWC}+S_{WL})/(S_{D1}+S_{WL}-S_{SR});$
$S_{WL}'=S_{SR}'=S_{D1}'=0; \quad S_A'=S_A-S_{D1}$

5.2.3 σ_{wf}, water flow

Outflows are computed by the simplest application of AMD.

5.2.4 $\sigma_{wie\&ld}$, water inclusion, extrusion and process of lahar complete deposition

When $p_{slt}<S_{KH}<p_{wct}$, water extrusion occurs, according an empirical approximate function "water loss": $\Delta S_{LWC} = f_{wl}(S_{KH}, p_{slt}, p_{wct})$, f_{wl} accounts for water extrusion in lahar and expresses linearly water content loss between two values of kinetic head p_{slt} and p_{wct}, considering that gravitational water content at p_{slt} is approximated to 0. When $S_{KH} \le p_{slt}$ lahar stops and complete deposition occurs: $\Delta S_A = S_{LT}$; $S_{LT}' = 0$; $S_{LWC}' = 0$, in the case of secondary lahars, intrusion of all the water of rainfall into the lahar is considered when $S_{KH} > p_{wct}$, S_{LWC} and S_{LT} increase proportionally to intruded water.

5.3 Simulation with LLUNPIY

Cotopaxi is a potentially active stratovolcano in the Andes Mountains, located about 50 km south of Quito, Ecuador, South America. The main danger of a huge eruption of Cotopaxi would be the flow of ice from its glacier with pyroclastic material. In the case of large eruption, it could destroy many settlements around the volcano. One of these is the city of Latacunga, which is located in the south-west valley and already destroyed in the 18th century (a village at that time) by volcanic activity [23, 24].

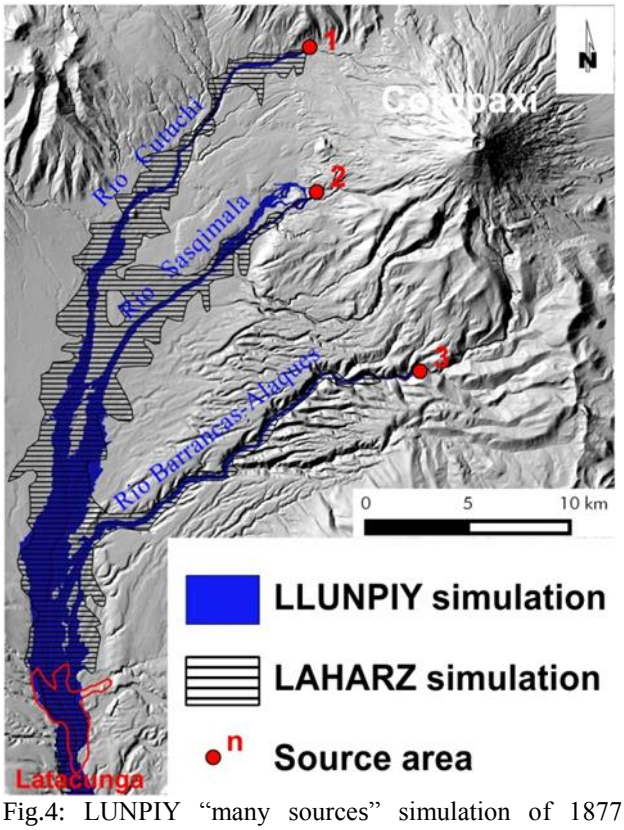

Fig.4: LUNPIY "many sources" simulation of 1877 lahars.

LLUNPIY model was applied to Cotopaxi 1877 event of primary lahars [23], after the successful simulation of some secondary lahars of Tungurahua volcano [19, 20]. We followed, as first approach, the

"many sources" simplification proposed in [24] that the main event could be equivalently generated, considering the initial positions of lahars sources in the three principal streams (Fig.4): Río Cutuchi, Río Sasqìmala and Río Barrancas-Alaques. In each of these three streams, we have placed, respectively, $18.5 \times [10]^6$ m^3, $9.5 \times [10]^6$ m^3 and $10 \times [10]^6$ m^3 of lahar matter.

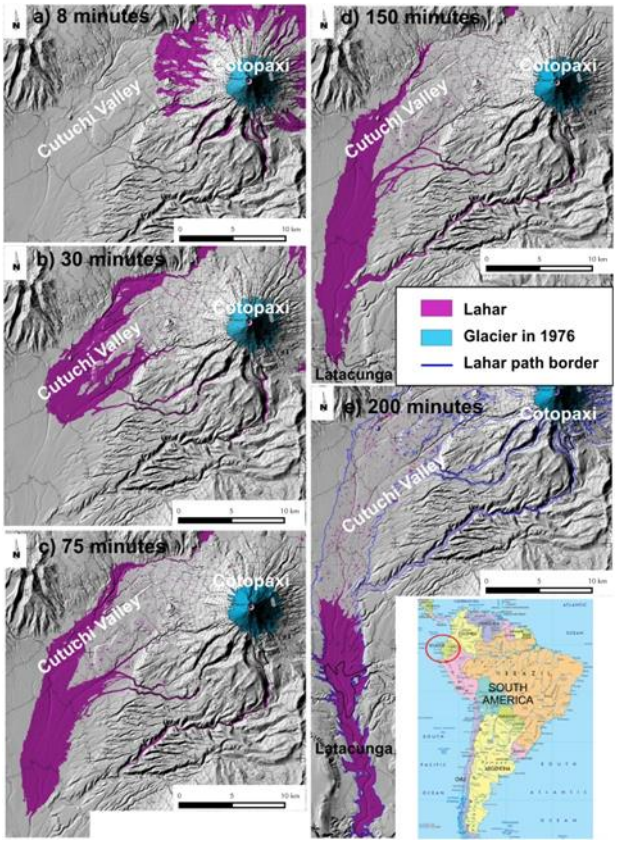

Fig.5: LLUNPIY "glacier melting" simulation of 1877 lahars.

The resultant simulations are shown in Fig.5. These results are comparable with simulations performed by the model LAHARZ [24], that considered larger quantities of initial lahars ($120 \times [10]^6$ m^3 sum of: $60 \times [10]^6$ m^3 in Río Cutuchi, $30 \times [10]^6$ m^3 in Río Sasqímala and $30 \times [10]^6$ m^3 in Río Barrancas-Alaques). The width of LLUNPIY simulation is smaller in the area next to "spurious" sources, but LAHARZ simulation is larger (Fig.4). The two results are very similar in the final sector (Latacunga area), because, at the end, the addition of eroded material in LLUNPIY balances the two approaches.

This CA approach involves the limit of initial quantity of lahar at the sources, because overflows can distort the effective evolution of the phenomenon. This did not permit to overcome an initial lahar quantity at the beginning in the previous simulation. For this purpose, we introduce a new CA "elementary process" of glacier melting. The ice layer is supposed to enclose pyroclastic matter and to melt immediately (the LLUNPIY first step) the glacier. That is more realistic than sources approach, if the rapid evolution of eruption is considered. The simulations of icecap melting are based on data, which correspond to 1976 glacier extension [8] with average glacier thickness of 50m. In the simulation, only 10m of ice is melt. Fig.5 shows the results of simulated event in various times. The paths are the same of "many source" simulation, but in the case of "glacier melting" widths are obviously larger. Results of simulation agree with partial data of the chronicles of that time [28]. Such a simulation could be considered a possible scenario for a future eruption of Cotopaxi because current DEM (Digital Elevation Model) was used together with measures of glacier extension.

4 Conclusion

The MCA methodological approach was applied in order to develop models of different fast moving surface flows of the type lahar and debris flow. Such models, SCIDDICA-SS2, SCIDDICA-SS3 and LLUNPIY present a similar structure that is differentiated in relation to the characteristics of the phenomenon; it implies the introduction of different and/or new elementary processes together with new sub-states and parameters. The common core regards the calculation of moving quantities from the central cells to the other cells of the neighboring; such outflows are idealized as "cylinders" tangent the next edge of the own hexagonal cell, according different motion equations; the different formulae based on the minimization algorithm determine quantity and direction of the outflows. MCA approach allows easily to introduce new elementary processes for refining or differentiating CA models.

SCIDDICA-SS3 represents a SCIDDICA-SS2 extension for cases, where a better approximation of momentum is necessary; in fact, some elementary processes were expanded.

LLUNPIY introduces new elementary processes that permitted to adequate the "common" elementary processes to lahar features and to introduce various triggering mechanisms that yielded to the new satisfying results concerning the 1877 lahars of Cotopaxi volcano, starting from simulation of the immediate melting of part of the Cotopaxi icecap.

Future research about lahar will continue with improving the triggering process, by considering the

ISBN: 978-1-61804-314-6

progressive glacier melting by pyroclastic bombs of volcanic eruptions for the Cotopaxi case.

References:

[1] M.V. Avolio, S. Di Gregorio, W. Spataro, G.A. Trunfio, A Theorem about the Algorithm of Minimization of Differences for Multicomponent Cellular Automata, *ACRI 2012*, LNCS 7495, Springer-Verlag Berlin, 2012, pp. 279–288.

[2] M.V. Avolio, G.M. Crisci, D. D'Ambrosio, S. Di Gregorio, G. Iovine, R. Rongo, W. Spataro, An extended notion of Cellular Automata for surface flows modelling, *WSEAS Transactions on Computers*, Vol. 4(2), 2003, pp. 1080-1085.

[3] M.V. Avolio, S. Di Gregorio, V. Lupiano, P. Mazzanti, W. Spataro, Application context of the SCIDDICA model family for simulations of flow-like landslides. In Proceedings international conference on scientific computing, Las Vegas (USA), 2010, pp. 40-46.

[4] M.V. Avolio, V. Lupiano, P. Mazzanti, S. Di Gregorio, An advanced Cellular Model for Flow-type Landslide with Simulations of Subaerial and Subaqueous cases, *Proceedings of 23rd EnviroInfo*, Vol.1, Shaker Verlag, Aachen, 2009, pp. 131-140.

[5] M.V. Avolio, V. Lupiano, P. Mazzanti, S. Di Gregorio, Modelling combined subaerial-subaqueous flow-like landslides by Cellular Automata. *In Cellular Automata*. Springer Berlin Heidelberg, 2008, pp. 329-336.

[6] M.V. Avolio, V. Lupiano, P. Mazzanti, S. Di Gregorio, SCIDDICA-SS3: A New Version of Cellular Automata Model for Simulating Fast Moving Landslides, J. Supercomput., Vol. 65, 2013, pp. 682-696.

[7] D. Barca, S. Di Gregorio, F.P. Nicoletta, M. Sorriso-Valvo, A cellular space model for flow type landslides. *In Computers and their Application for Development. Proc. Int. Symp. IASTED (Taormina)*. 1986. p. 30-32.

[8] B. Cáceres, J. Ramírez, B. Francou, J.P. Eissen, J.D. Taupin, E. Jordan, L. Ungerechts, L. Maisincho, D. Barba, E. Cadier, R. Bucher, A. Peñafiel, P. Samaniego, P. Mothes, Determinación del volumen del casquete de hielo del volcán Cotopaxi. *Informe INAMHI, IRD, IG-EPN, INGEOMINAS*, 2004.

[9] B. Chopard, Cellular automata modeling of physical systems. *Computational Complexity: Theory, Techniques, and Applications*, 2012, pp. 407-433.

[10] A. Clerici, S. Perego, Simulation of the Parma River blockage by the Corniglio landslide (Northern Italy). *Geomorphology*, 2000, vol. 33, no 1, pp. 1-23.

[11] G.M. Crisci, S. Di Gregorio, R. Rongo, W. Spataro, PYR: a Cellular Automata model for pyroclastic flows and application to the 1991 Mt. Pinatubo eruption. *Future Generation Computer Systems*, vol. 21, no 7, 2005, pp. 1019-1032.

[12] G.M. Crisci, M.V. Avolio, B. Behncke, D. D'Ambrosio, S. Di Gregorio, V. Lupiano, M. Neri, R. Rongo, W. Spataro, Predicting the impact of lava flows at Mount Etna, Italy. *J. Geophys.* Res., Vol. 115, 2010, pp 1-14.

[13] D. D'Ambrosio, S. Di Gregorio, S. Gabriele, R. Gaudio, A Cellular Automata Model for Soil Erosion by Water. *Physics and Chemistry of the Earth, Part B: Hydrology, Oceans and Atmosphere*, vol. 26, no 1, 2001, pp. 33-39.

[14] S. Di Gregorio, R. Serra, An empirical method for modelling and simulating some complex macroscopic phenomena by cellular automata, *Future Generation Computer Systems* Vol.16, No2/3, 1999, pp. 259-271.

[15] U. Frisch, D. D'Humieres, B. Hasslacher, P. Lallemand, Y. Pomeau, J.P. Rivet, Lattice gas hydrodynamics in two and three dimensions. *Complex Systems* 1, 1990, pp. 649-707.

[16] B. Hayes, The cellular automaton offers a model of the world and a world unto itself. *Scientific American*, 250(3), 1984, pp.12-21.

[17] V. Lupiano, M. V. Avolio, M. Anzidei, G.M. Crisci, S. Di Gregorio, Susceptibility Assessment of Subaerial (and/or) Subaqueous Debris-Flows in Archaeological Sites, Using a Cellular Model. *In Engineering Geology for Society and Territory-Volume 8*. Springer International Publishing, 2015, pp. 405-408.

[18] V. Lupiano, M. V. Avolio, S. Di Gregorio, D.J. Peres, L. M. Stancanelli, Simulation of 2009 debris flows in the Peloritani Mountains area by SCIDDICA-SS3. *Proceeding of 7th WSEAS International Conference on Engineering Mechanics, Structures, Engineering Geology*, Salerno (Italy), 2014b, pp. 53-61, ISBN: 978-960-474-376-6.

[19] G. Machado, V. Lupiano, G. M. Crisci and S. Di Gregorio, LLUNPIY Preliminary Extension for Simulating Primary Lahars Application to the 1877 Cataclysmic Event of Cotopaxi Volcano to be published in Proceedings of SIMULTECH, 2015.

[20] G. Machado, V. Lupiano, M.V. Avolio, F. Gullace, S. Di Gregorio, A cellular model for

secondary lahars and simulation of cases in the Vascún Valley, Ecuador. Submitted to Journal of Computational Science, 2015.

[21] G. Machado, V. Lupiano, M.V. Avolio, S. Di Gregorio, A Preliminary Cellular Model for Secondary Lahars and Simulation of 2005 Case of Vascún Valley, Ecuador. In *Proceeding ACRI 2014 International Conference, LNCS 8751 Springer International Publishing*, 2014, pp. 208-217

[22] P. Mazzanti, Bozzano F., Avolio M.V., Lupiano V., Di Gregorio S.: 3D numerical modelling of submerged and coastal landslides propagation, Advances in Natural and Technological Hazards Research, Vol.28, Springer Verlag, Berlin, 2010. pp. 127-138.

[23] P. Mothes, J.W. Vallance, Volcanic Hazards, Risks, and Disasters, In Lahars at Cotopaxi and Tungurahua Volcanoes, Ecuador, *Elsevier Inc*., New York, 2014, pp.141-167.

[24] M. Pistolesi, R. Cioni, M. Rosi, E. Aguilera, Lahar hazard assessment in the southern drainage system of Cotopaxi Volcano, Ecuador: Results from multiscale lahar simulations. *Geomorphology* 207, 2014, pp. 51-63.

[25] T. Salles, S. Lopez, M.C. Cacas, T. Mulder, Cellular automata model of density currents. *Geomorphology*, Vol.88, 2007, pp. 1-20.

[26] S. Succi, *The Lattice-Boltzmann Equation*. Oxford university press, Oxford, 2001.

[27] J. von Neumann, Theory of self-reproducing automata. Edited and completed by Arthur W. Burks. *Illinois University Press*, 1966.

[28] T. Wolf, Memoria sobre el Cotopaxi y su Última Erupción Acaecida el 26 de Junio de 1877. *Imprenta del Comercio, Guayaquil, Ecuador*, 1878